

Helicity correlated asymmetries caused by optical imperfections

K. Aulenbacher^a

For the A4 Collaboration
Institut für Kernphysik, Johannes-Gutenberg Universität Mainz, D-55099 Mainz, Germany

Received: 31 August 2006

Published online: 14 June 2007 – © Società Italiana di Fisica / Springer-Verlag 2007

Abstract. False asymmetries in electron scattering experiments utilizing photoelectron sources are generated by imperfections of the light polarization optics. The false asymmetries are amplified by an analyzing power of the photocathodes. We have demonstrated compensation techniques which allow to approach zero intensity asymmetry with good stability. Even in the absence of analyzing powers fluctuations may be generated by more subtle effects like varying interference patterns of the exciting laser beam.

PACS. 42.25.Ja Polarization – 78.20.Jq Electrooptical effects

1 Introduction

Scattering experiments may attempt to measure the parity-violating (PV) asymmetry A_z

$$A_z = \frac{\sigma^+ - \sigma^-}{\sigma^+ + \sigma^-}. \quad (1)$$

Here σ^\pm denotes the cross-section for a positive or negative helicity of the particle beam which moves along the z -direction onto an unpolarized target. The σ^\pm are usually differential cross-sections which are determined from the rates R^\pm measured by a detection system which is placed under a suitable angle with respect to the z -direction. In a first approximation the rates are proportional to the cross-section $R^\pm = f(\mathbf{x}^\pm)\sigma^\pm$. The function $f(\mathbf{x}^\pm)$ depends on a vector $\mathbf{x}^\pm = x_1^\pm, \dots, x_N^\pm$ with N parameters. These in particular include the beam parameters (intensity I , position on target (x, y) , angle at target (x', y') ...). If all parameters are independent of the helicity state $(x_1^+, \dots, x_N^+) = (x_1^-, \dots, x_N^-)$ it follows that the asymmetry A_z is equal to the measured rate asymmetry $A_R = (R^+ - R^-)/(R^+ + R^-)$ since the function $f(\mathbf{x}^\pm)$ cancels out. If this is not the case A_R is approximately given by

$$A_R \approx A_z + \sum_i \chi_i \Delta x_i = A_z + A_{false}. \quad (2)$$

$\Delta x_i = x_i^+ - x_i^-$ is the helicity-correlated (HC) fluctuation of the i -th parameter and $\chi_i = (df(\mathbf{x})/dx_i)|_{\mathbf{x}}/f(\mathbf{x})$ represents the sensitivity of the rate asymmetry on the fluctuation of the i -th parameter. Since A_z has to be extracted from A_R the sum over the HC fluctuations has

to be controlled in such a manner that the uncertainty of A_{false} is within the desired error budget. It should be kept in mind that A_z is typically of the order of 10^{-6} so that an accuracy goal of, *e.g.*, 10% leads to the requirement that the error in the determination of A_{false} must be below 100 ppb. To achieve this several issues emerge from an inspection of eq. (2). First, the sensitivities have to be known. Second, because the χ_i can only be determined with limited accuracy, the Δx_i must be kept small and, in addition, they themselves have to be measured with sufficient accuracy.

In all present day electron scattering PV experiments helicity switching is done by generating and reversing the circular polarization of a laser beam by a Pockels cell. The circularly polarized light is then used to produce electrons of alternating spin polarization (beam intensity I^\pm) via photoeffect from suitable semiconductor heterostructures like strained GaAs [1,2] or superlattices [3]. All types of photocathodes presently utilized exhibit a non-vanishing analyzing power with respect to linear light polarization components [4,5]. On the other hand, HC linear polarization fluctuations are virtually unavoidable because of optical imperfections. This is the dominant reason for the appearance of a beam intensity asymmetry

$$A_I = \frac{I^+ - I^-}{I^+ + I^-}. \quad (3)$$

It is the main contribution to A_{false} if no precautions are taken.

In the following section A_I is analyzed for the case of the PVA4 experiment at the MAMI accelerator in Mainz. It will be shown that the observed intensity asymmetry can be reliably compensated and its dependence on the parameters of the optical system is reasonably well under-

^a e-mail: aulenbac@kph.uni-mainz.de

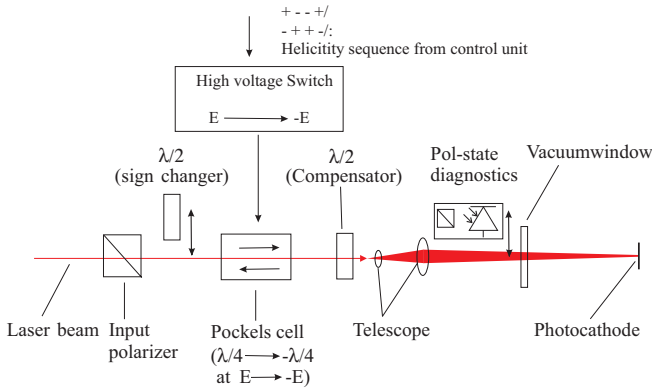


Fig. 1. Polarization optics for PVA4 (schematic).

stood. Section 3 provides additional investigations which for example demonstrate the existence of HC beam position fluctuations even in the absence of an analyzing power of the photocathode. The acceleration process may then map this variation onto HC fluctuations of all other beam parameters. Finally, the last section summarizes the present accuracy of the determination of false asymmetries for the PVA4 experiment at Mainz.

2 Optical imperfections and HC asymmetries

2.1 Polarization optics for the PVA4 experiment

The laser system of the Mainz polarized source has been described elsewhere [6]. An almost perfect linear polarization is achieved from the collimated laser beam after passing the input polarizer (fig. 1). The Pockels cell is oriented in a way that its electrically controlled optical axis is at 45 degree with respect to the linear polarization. If the phase shift of the cell is adjusted to $\pi/2$ ($-\pi/2$) positive (negative) circular polarization is generated. The phase shift ϕ is proportional to the applied voltage, $\phi^\pm = \pm\pi/2$ is achieved at ± 2800 V. The beam diameter in the cell is about 2 mm.

A control device generates a continuous sequence of \pm state signals which is transferred to corresponding circular light polarization by the Pockels cell and its high-voltage switch (fig. 1). The pattern for four 20 ms long states is either $(- + + -)$ or $(+ - - +)$. After a four pattern is completed the first sign of the next pattern is determined at random. The state sequence is also transmitted to the PVA4 data acquisition. The measurement of all parameters contributing to eq. (2) is synchronized to the state sequence thus allowing to measure the HC fluctuations at a rate of 25 Hz.

An insertable half-wave plate (“sign changer”) is used to rotate the input polarization by $\pi/2$, which changes the sign of helicity with respect to the control sequence. The physical asymmetry (A_z) then changes sign, whereas for example the false asymmetry resulting from an unequal length of the $+/-$ state will not. The observation of a sign change is therefore an important experimental check.

Behind the Pockels cell the beam passes another half-wave plate which is rotatable around the beam axis. It serves as a compensator for A_I (see sect. 2.3). The following telescope focuses the beam onto the photocathode to a spot of 0.3 mm diameter. Before hitting the cathode the laser beam has to pass a vacuum window which is located about 1.5 m in front of the photocathode.

Between telescope and vacuum window an insertable rotating polarizer/photodetector combination allows to determine the degree of circular polarization. A circular polarization of $P_\sigma^\pm \geq \pm 0.998$ is routinely achieved.

2.2 Residual linear polarization and compensation

Residual linear polarization components may perform HC variations by 90 degree if the asymmetric phase shift of the Pockels cell is non-zero

$$\Delta\phi_{PC}^a = (\phi^+ + \phi^-)/2 \neq 0. \quad (4)$$

As an extreme example one can imagine to arrange for phase shifts of the Pockels cell which are $\phi^+ = 0$ and $\phi^- = -\pi$. In this case the linear input polarization is not changed at all in the first case and it is rotated by 90 degree in the second. In a real experiment the asymmetry of the phase shift will of course be minimized but the residual linear polarization will always contribute. An upper limit for residual linear polarization is given by the relation

$$P_\sigma^2 + P_{lin}^2 \leq 1. \quad (5)$$

For our case ($P_\sigma > 0.998$) P_{lin} may be as large as 0.06.

Only a small fraction of the light intensity is absorbed in the active regions of the photocathodes presently in use for PV experiments [1]. The absorption coefficient of these photocathodes varies with the orientation of the linear polarization as in an imperfect dichroic polarizer [4]. Since the emission current is proportional to the absorbed light intensity a corresponding modulation of the emission current with respect to a rotation of polarization will be observed. The amplitude of this modulation (for completely polarized light) is called the analyzing power. Photocathodes used for PVA4 exhibited a typical analyzing power of $\kappa = 3.5\%$. Since helicity switching generates a 90 degree rotation of the residual linear components a non-zero HC beam intensity asymmetry (A_I) of the order of $\kappa P_{lin} \approx 2000$ ppm is typically observed which is far from being acceptable.

The role of the compensator half-wave plate in fig. 1 is in principle the following: If the orientation of its fast axis with respect to the residual linear polarization components is given by an angle β it will rotate them by 2β (its action on the circular components is an additional sign change). Since the cathode “polarizer” has a 180 degree periodicity it follows that the beam intensity gets modulated around an average value \bar{I} like $I^\pm = \bar{I}(1 \pm \kappa P_{lin} \cos(4\beta))$. A_I will then vanish for example at $\beta = \pi/8$.

2.3 Quantitative analysis of A_I

A_I can be calculated by using polarization transfer matrices that take into account realistic (*i.e.* imperfect) optical elements. A detailed description of this method is provided in a paper by Humensky *et al.* [7]. In this article we restrict ourselves to a brief outline and a presentation of the results at PVA4.

The polarization transfer matrices may act on the Stokes vector (Mueller matrices) or on the field amplitudes (Jones matrices). In our case the optical elements are either retarders (*e.g.*, Pockels cell) or polarizers (cathode). It is assumed that the optical elements between the input polarizer and the cathode are birefringent with retardations $\phi_{element}$ and have an orientation of their optical axis with respect to the input polarization given by angles $\theta_{element}$. The only imperfections taken into account are deviations from the nominal phase shifts $\Delta\phi_{element}$ and misalignments of the optical axis $\Delta\theta_{element}$. Stokes vectors behind the Pockels cell are helicity dependent, so that they carry the index \pm .

It is then possible to calculate the Stokes vector behind the active region of the cathode (S_{cath}^{\pm}) by consecutive application of the individual element matrices to the input Stokes vector S_{in} in front of the Pockels cell. The first vector component $S_{cath,0}^{\pm}$ corresponds to the transmitted intensity — which of course also defines the absorbed intensity and therefore the emission current. Using the matrices given in [8] we can therefore obtain the intensity asymmetry as a function of the matrix elements. The elements are approximated up to the first order with respect to the imperfections. A_I also depends on two additional variables β and θ_C which are the compensator angle and orientation of the cathode taken with respect to the input polarization. The resulting asymmetry is a special case of a more general form presented in [7] and can be written as

$$A_I = \kappa [\Delta\phi_{PC}^a \cos(2\theta_c - 4\beta) - \Delta\phi_C \sin(2\theta_c - 2\beta) + \Delta\phi_{optic} \sin(2\theta_c + 2\Delta\theta_{optic})]. \quad (6)$$

$\Delta\phi_{PC}^a$ is the asymmetric phase shift of the cell (eq. (4)). $\Delta\phi_C$ is the deviation of the compensator phase shift from its nominal half-wave retardation. The effective birefringence of telescope and vacuum window is taken into account by $\Delta\phi_{optic}$ and $\Delta\theta_{optic}$ (the nominal value would be $\phi_{optic} = 0, \theta_{optic} = 0$). The summands of eq. (6) are named according to their β -dependence as the “ 4β ”, “ 2β ” and “offset” (β -independent) terms with their corresponding amplitudes $\kappa\Delta\phi_{PC}^a$, $\kappa\Delta\phi_C$ and $\kappa\Delta\phi_{optic}$.

2.4 Experimental result for A_I

Figure 2 shows a measurement of A_I with respect to a variation of the compensator angle at fixed cathode orientation. The fit function has two additional free phases since the orientation of the cathode “polarizer” and of the half-wave plate with respect to input polarization were unknown. From the amplitudes determined by the fit we find the following values for the imperfections.

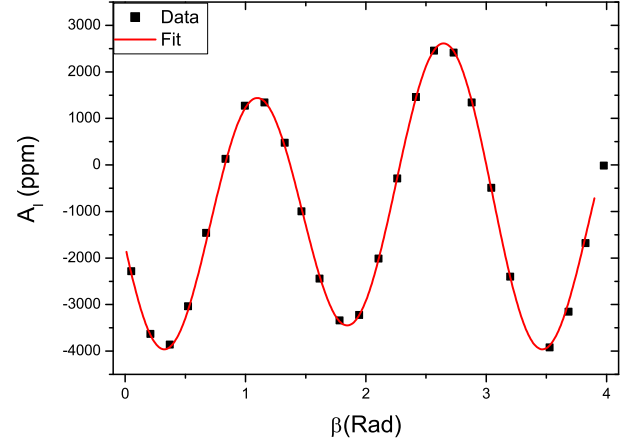


Fig. 2. A_I measurement at PVA4 target with fit.

- The 2β summand contributes with an amplitude of ≈ 640 ppm yielding $\Delta\phi_C = 18$ mrad, which is within the specifications of the half-wave plate.
- The 4β amplitude is approximately 2860 ppm, yielding $\Delta\phi_{PC}^a = 81$ mrad. The large value has been created mostly on purpose because no zero crossing of the A_I -curve may be obtained if $\kappa\Delta\phi_{PC}^a$ is too small with respect to the offset term. The Pockels cell was operated with asymmetric voltages (+2900/−2700 V) which will result in $\Delta\phi_{PC}^a = 58$ mrad. The remaining deviation from the observation (23 mrad) is probably generated by a residual phase offset, *e.g.* strain-induced birefringence in the Pockels crystal.
- The offset term contributes about −830 ppm in this measurement. Since the angle $2\theta_c + 2\Delta\theta_{optic}$ was unknown $\Delta\phi_{optic}$ had to be determined by a separate measurement and is estimated to be ≈ 70 mrad (see sect. 2.5). A major contribution to this birefringence comes from the vacuum window.

Rotating the compensator to a zero crossing of A_I defines a condition which is suitable for data taking during PVA4. Its noteworthy that A_I does not (in first order) depend on the symmetric deviation of the phase shift ($\Delta\phi_{PC}^s = (\phi^+ - \phi^- - \pi)/2$). An example for such a symmetric deviation is the thermal phase drift of our KD*P Pockels cell which is $\approx -3\%/K$. Its influence on the temporal stability of the compensation is therefore suppressed.

2.5 Offset compensation

It is necessary to have non-zero errors $\Delta\phi_{PC}^a$ and $\Delta\phi_C$ to compensate for the offset term. The slope of the zero crossing determines the stability and accuracy of setting A_I to zero. Therefore it is desirable to minimize the offset term which then in turn would allow to minimize the other errors. Since the offset is $\propto \sin(2\theta_c + 2\Delta\theta_{optics})$ it can be compensated by changing θ_c which is possible in our set up because the cathode can be rotated under vacuum. We have therefore performed an experiment during which

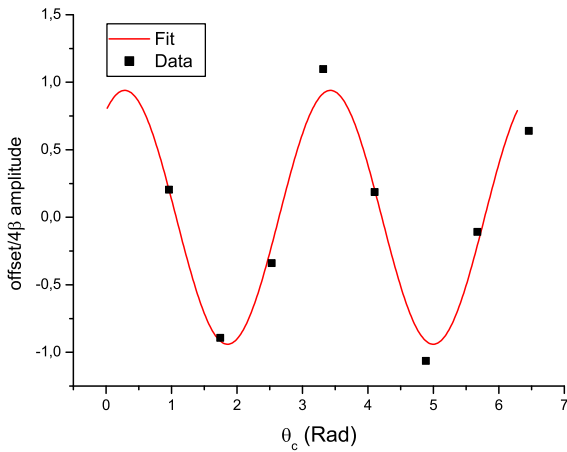


Fig. 3. Measurement of the offset/ 4β ratio as a function of θ_c .

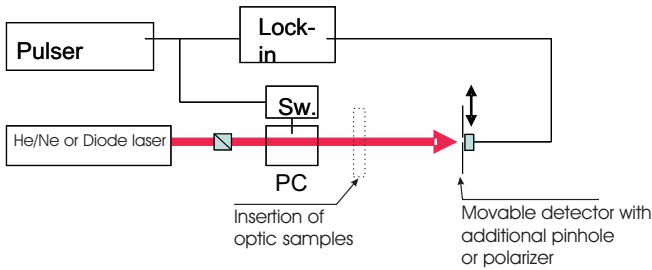


Fig. 4. Testbench for optical components.

$A_I(\beta)$ was measured for various angles θ_c . The summands entering in eq. (6) were determined for each angle. Figure 3 shows the ratio of the offset term and the 4β amplitude as a function of θ_c . The expected $2\theta_c$ variation and the expected zero crossings is clearly demonstrated.

From the maximum offset contribution observed in this measurement (2500 ppm) we can infer the total birefringent phase shift of the optics between Pockels cell and cathode to $\Delta\phi_{\text{optic}} = 70$ mrad.

3 Other HC asymmetries

Several observations which are relevant for false asymmetries were made with the help of the set-up shown in fig. 4. A high-voltage switch is triggered by a square wave signal generated by pulse generator. The switch forces the Pockels cell to change circular polarization synchronous to the square wave. A HC photodetector current is then phase locked to the pulser signal and detected by a lock in the amplifier. $A_I < 10^{-4}$ can be reliably measured within a few seconds, thus allowing for fast variation of parameters. In all cases the cell was carefully adjusted and the beam was centered in the cell with an accuracy of ≈ 0.2 mm.

3.1 A_I with minimized analyzing power

A_I was measured without elements between the Pockels cell and the detector. The analyzing power of the detector



Fig. 5. Backreflection for the different helicity states.

was measured to be $< 10^{-2}$, leading to the expectation of a very small A_I . The experiment is therefore less sensitive to changes of the polarization state but detects HC changes of the light intensity. This situation is similar to early PV electron scattering experiments which were carried out with bulk-GaAs photocathodes. Bulk-GaAs also has a low analyzing power [5]. To promote this approach a HeNe laser was used to obtain better beam quality. Surprisingly an enormous asymmetry $A_I = 1\%$ was observed. An inspection of the backreflections from the cell windows revealed that their modulation was even larger. Since the windows are tilted by a small angle with respect to the Pockels crystal¹ the reflections can be separated from the main beam (fig. 5). The average intensity in fig. 5 is 10% of the transmitted intensity and A_I^R (R for reflected) is also 10%, leading to $A_I^T = -0.01$ for the transmitted beam in agreement with the observation. If an infrared (IR) laser diode is used instead of the HeNe—in this case the reflected intensity is $< 1\%$ because the Pockels cell is antireflection coated for IR—the asymmetry shrinks to $A_I^T < 100$ ppm.

3.2 Investigation of birefringence of inserted elements

In this case a polarizer was mounted in front of the detector in order to maximize the sensitivity according to eq. (6) ($\kappa = 1$) and rotated to obtain the parameter $\Delta\phi_{\text{optic}}$. The total $\Delta\phi_{\text{optic}}$ of a PVA4-type telescope and vacuum window was measured to 25 mrad. The largest contribution is caused by the vacuum window. We did not test the window under vacuum conditions but it seems probable that its effect will increase because of strain-induced birefringence. This may explain the difference to the 70 mrad observed at the PVA4 set-up.

3.3 Spatially resolved HC fluctuations

The detector was covered by a $25\ \mu\text{m}$ pinhole and was moved transverse to the direction of the laser beam (x -direction). No optical elements were introduced between Pockels cell and the pinhole therefore again minimizing the analyzing power of the system behind the Pockels cell. Possible reasons for HC beam movements in the presence of an analyzing power are discussed in [7].

Figure 6 shows the resulting distributions for intensity $I(x)$ and $A_I(x)$. An IR laser diode was used simulating

¹ A precaution of the manufacturer against optical feedback.

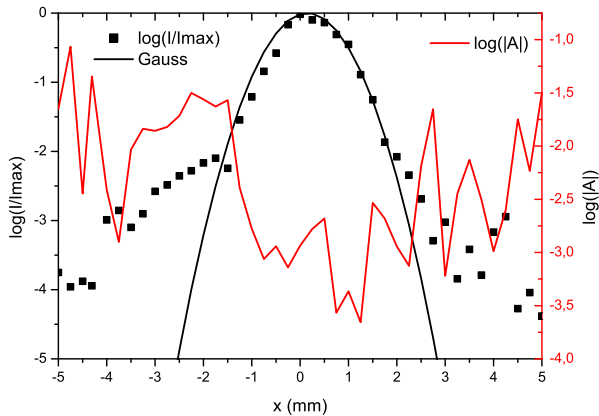


Fig. 6. Measurement of $A_I(x)$.

realistic PVA4 operating conditions. It can be seen that $I(x)$ in the beam center is approximately Gaussian with an $1/e^2$ diameter of 2.4 mm. At radii > 2 mm the intensity distribution is dominated by a superimposed halo. Since the distribution $A_I(x)$ is asymmetric (the largest values are found in the halo to the left) a HC movement of the beam centroid $\langle x \rangle$ is observed, for the data in fig. 6 we find $\Delta\langle x \rangle = 1 \mu\text{m}$.

3.4 Interpretation of the effects

The HC asymmetries presented in 3.1 and 3.3 are caused by a modulation of the light intensity at the detector.

The first effect could be explained by interference between the beams reflected from the front and the backwindow of the cell. Since these are separated longitudinally the temporal coherence length of the laser device is important (see also [7]). The HeNe laser has a much larger coherence length if compared to the IR diode. Therefore it's not surprising that the reduction of A_I observed when changing from HeNe to IR diode ($\approx 1/100$) is larger than the reduction of reflected intensity ($\approx 1/10$).

The spatial modulation of intensity with helicity within the halo of the laser beam (fig. 6) may also be a (transverse) coherence effect. It seems probable that polarization states of the halo have much larger linear components with 90 degree flip than the main beam. Since the interference pattern can even disappear completely if one of two interfering beams rotates its (complete) linear polarization by 90 degree (see [8], p. 256) it seems possible that large A_I values in the beam halo are generated by this mechanism. HC beam steering is probably not the reason because of the missing symmetry in the data.

3.5 Couplings

The results presented in fig. 6 lead to a HC movement of the beam section of $1 \mu\text{m}$. Taking into account a possible averaging out of the effect for the whole two-dimensional distribution and the strong demagnification of the beam

Table 1. Correction for false asymmetries and resulting errors for PVA4 measurement at $Q^2 = 0.108 (\text{GeV}/c)^2$ [9].

Parameter	Correction (ppb)	Error (ppb)
Current A_I	330	40
Position $A_{x,y}$	10	90
Angle $A_{x',y'}$	10	90
Energy A_E	30	30

size by the telescope (fig. 1) we estimate the HC movement on the cathode to be about one order of magnitude smaller, *i.e.* 100 nm. Such a movement couples to angular variations due to the focusing elements of the electron optics. With a focusing strength of 1m^{-1} (typical strength in the 100 keV injection system of the polarized source at MAMI) this transforms into 100 nrad HC angular variation. In addition, an angular variation can lead to path length differences which change the acceleration in the (*e.g.*) third microtron stage of MAMI and therefore lead to a HC energy variation which is estimated to be $\approx 5 \cdot 10^{-9}$. Therefore all beam parameters at the target may show HC fluctuations what is indeed observed at the PVA4 target with the expected order of magnitude.

4 Conclusion: false asymmetries at PVA4

Table 1 shows final values of false asymmetries obtained during the 570 MeV PVA4 experiment [9]. A_I was minimized to 330 ppb with the technique described in sect. 2.3, for the other parameters a decreasing effect of the stabilization systems which work on the uncorrelated parameter fluctuations proved sufficient. It can be seen that angular and position fluctuations do both contribute 90 ppb to the error, which is small against the statistical error (290 ppb). Nevertheless, we envisage an active HC feedback system to compensate for the beam movement on the photocathode.

This work was supported by the Deutsche Forschungsgemeinschaft (DFG) within the framework of the Sonderforschungsbereich SFB-443.

References

1. T. Maruyama *et al.*, Phys. Rev. Lett. **66**, 2376 (1991).
2. T. Nakanishi *et al.*, Phys. Lett. A **158**, 345 (1991).
3. T. Omori *et al.*, Phys. Rev. Lett. **67**, 3294 (1991).
4. R.A. Mair *et al.*, Phys. Lett. A **212**, 231 (1996).
5. K. Aulenbacher *et al.*, *Proceedings of the Low Energy Polarized Electron Workshop, LE98* (SPES-Lab-publishing, St. Petersburg, 1998) p. 87.
6. K. Aulenbacher *et al.*, *Proceedings of the 6th European Particle Accelerator Conference, Stockholm 1998* (Institute of Physics Publishing, Bristol, 1998) p. 1388.
7. T.B. Humensky *et al.*, Nucl. Instrum. Methods A **512**, 261 (2004).
8. E. Collett, *Polarized light* (Dekker, New York, 1993).
9. F.E. Maas *et al.*, Phys. Rev. Lett. **94**, 152001 (2005).